Spiral CT of the temporal bone in unsedated pediatric patients.

G D Luker, B C Lee and K K Erickson

AJNR Am J Neuroradiol 1993, 14 (5) 1145-1150
http://www.ajnr.org/content/14/5/1145

Spiral CT of the Temporal Bone in Unsedated Pediatric Patients

Gary D. Luker, Benjamin C. P. Lee, and Kavita K. Erickson,

PURPOSE: To determine the feasibility of performing rapid, high-resolution, low-radiation–dose spiral CT scans of the temporal bone in unsedated pediatric patients. **METHODS:** Axial spiral CT examinations with an effective section thickness of 1.25 mm were performed in 41 infants and children. Multiplanar reconstructions were generated using 360° and 180° linear interpolation algorithms. Three-dimensional reconstructions of the middle ear were also performed. **RESULTS:** Complete axial spiral scans were performed without sedation in all patients. Three hundred sixty-degree linear interpolation images had comparable resolution to conventional CT; 180° linear interpolation images with an effective section thickness of 1.0 mm at 0.2-mm intervals showed good detail of middle and inner ear anatomy, and multiplanar reconstructions from this algorithm were comparable to direct scans. Three-dimensional reconstructions clearly displayed the oval window, malleus, and incus. **CONCLUSION:** Spiral CT is a clinically feasible method for rapidly evaluating the temporal bone in pediatric patients, eliminating the need for sedation. The images obtained from this technique are comparable to conventional CT. High-quality multiplanar reconstructions can be generated from the spiral data set, providing an alternative to direct scans in multiple planes. Additionally, three-dimensional images of internal temporal bone anatomy can be generated from the spiral data.

Index terms: Computed tomography, in infants and children; Computed tomography, technique; Temporal bone, computed tomography; Pediatric neuroradiology

AJNR 14:1145–1150, Sep/Oct 1993

High-resolution, multisection computed tomography (CT) has become the standard for temporal bone imaging (1). This conventional CT technique delivers a relatively high dose of radiation to the lens, particularly when scans are performed in multiple planes (2). In addition, sedation, which is required to eliminate motion in pediatric patients, has inherent morbidity and mortality.

The spiral CT technique is a rapid means of acquiring CT data and has proved effective in reducing problems associated with patient motion. In this study we aim to determine the feasibility of performing rapid, high-resolution, low-radiation spiral CT scans of the temporal bone in unsedated children. We compared the resolution of these scans and two-dimensional (2D) multiplanar reconstructions from spiral data with those acquired by conventional CT techniques. The capability of three-dimensional (3D) reconstructions to display the middle and inner ear is also evaluated.

Materials and Methods

The temporal bones were examined by the spiral CT technique in 41 infants and children (24 boys and 17 girls) with known or suspected temporal bone abnormalities. Fifteen had infections involving the middle ear; 12 were evaluated for a cochlear implant; six had congenital abnormalities; six were evaluated for trauma; and two had metastatic disease. The ages of the patients ranged from 3 months to 10 years. Eleven patients were younger than 2 years old; 13 were between 2 and 5 years old; and 17 were between the ages of 5 and 10 years.

All patients were evaluated between February 1, 1992, and October 31, 1992. Examinations were performed without sedation using the same Siemens Somatom Plus S scanner (Siemens Medical Systems, Iselin, NJ). For younger patients (generally younger than 2 years of age), a parent

Received January 25, 1993; revision received April 21 and accepted May 5.

Partial support was provided by Siemens Medical Systems.

All authors: Mallinckrodt Institute of Radiology, 510 South Kingshighway, St. Louis, MO 63110. Address reprint requests to Benjamin C. P. Lee, MD.

[1] Current Address: Ernst Radiology, Inc, 3450 Bridgeland, Bridgeton, MO 63044.

AJNR 14:1145–1150, Sep/Oct 1993 0195-6108/93/1405–1145

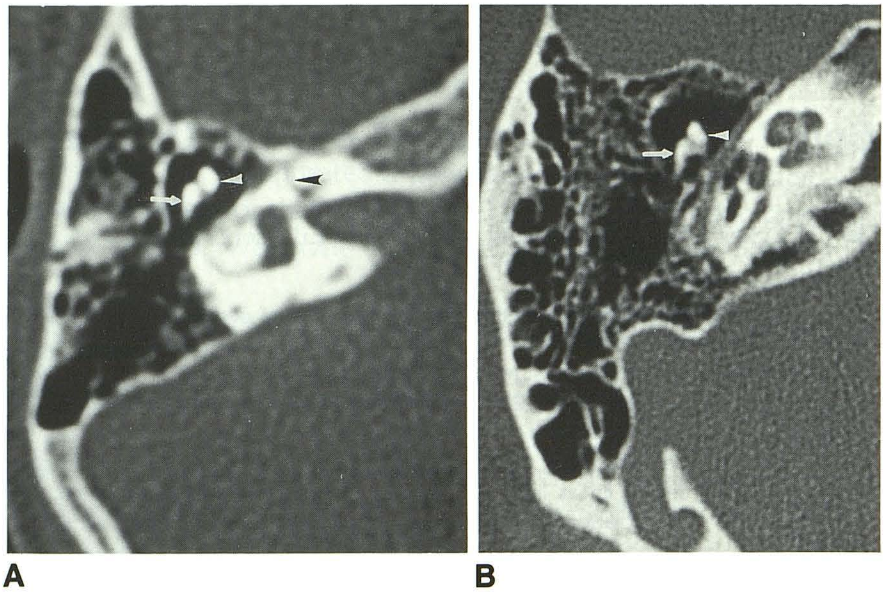

Fig. 1. Comparison of direct axial scans showing the head of the malleus (*white arrowhead*), short process of the incus (*white arrow*), and labyrinthine portion of the facial nerve canal (*black arrowhead*).

A, Spiral technique (1.25-mm effective section thickness).

B, Conventional technique (1-mm section thickness). Only a minimal loss of sharpness of the bone margins is seen with the spiral technique.

remained with the child during the scan to help immobilize the child's head. Standard scan parameters included a table speed of 1 mm/second for 30 seconds, 165 mA (4.95 A), and a high-resolution bone algorithm. In all patients, scans were acquired routinely in the axial plane with an effective section thickness of 1.25 mm. Using the original spiral CT data, coronal and sagittal reconstructions (contiguous 1.25-mm-thick sections) were generated for all patients. These reconstructions routinely were made using contiguous axial sections generated with a 360° linear interpolation algorithm. Additionally, submillimeter section images were constructed from the original spiral data using a 180° linear interpolation algorithm in 12 patients. The submillimeter images each have an effective section thickness of 1.0 mm. Contiguous images overlapped by 0.2 mm.

Conventional CT scans in the axial or coronal planes were performed in 12 patients for comparison with the spiral images. The conventional scans were performed using contiguous 1-mm sections at 220 mA and a high-resolution bone algorithm. In eight patients, direct coronal spiral examinations were done using the same parameters as described for the axial spiral scans. Data from the direct coronal spiral scans were reconstructed using both the 360° (1.25-mm effective section thickness) and 180° (1.0-mm effective section thickness with 0.2-mm image overlap) linear interpolation algorithms for comparison with the reconstructed coronal images from axial spiral data.

In six patients, 3D reconstructions from the original spiral projection data, tailored to display the ossicles and oval window, were performed. These reconstructions were generated using the standard surface-rendering 3D program available on the Somatom Plus S. A threshold value of 180 HU was empirically selected to optimize the osseus structures, and the appearance of depth was controlled by varying the direction of lighting on the image. The region of interest for the 3D images was selected from the nonreconstructed scans using the boundaries described by Howard et al (3). Using interactive controls, bone was then successively cut away from the original 3D surface rendering until the ossicles and oval window were identified. The image was rotated about the x, y, and z axes to display best the middle-ear structures. Approximately 5 minutes were typically required to generate these 3D images. Additionally, 3D images using the submillimeter data from spiral scans were generated in two patients.

Results

Complete axial evaluations of the temporal bone were successfully performed in all 41 patients. This included seven patients with whom parents were present to hold the head and eliminate motion. Apart from a minimal loss of sharpness of the ossicular margins, the direct spiral axial and coronal images using 360° linear interpolation (1.25-mm effective section thickness) were subjectively judged to be comparable to the conventional single-section CT images. The round and oval windows, ossicles, and facial nerve canals could be readily identified on all of the spiral examinations (Figs 1 and 2). All pertinent anatomy and disease demonstrated on the conventional scans were also clearly seen on the spiral images. These findings included opacities in the mastoids and middle ear, as well as bone destruction from a rhabdomyosarcoma (Fig 3). Submillimeter axial reconstructions with 180° linear interpolation (effective section thickness of 1.0 mm with 0.2-mm image overlap) provided detailed images of the temporal bone internal anatomy (Fig 4).

The 1.25-mm section thickness coronal reconstructions from axial spiral data showed some

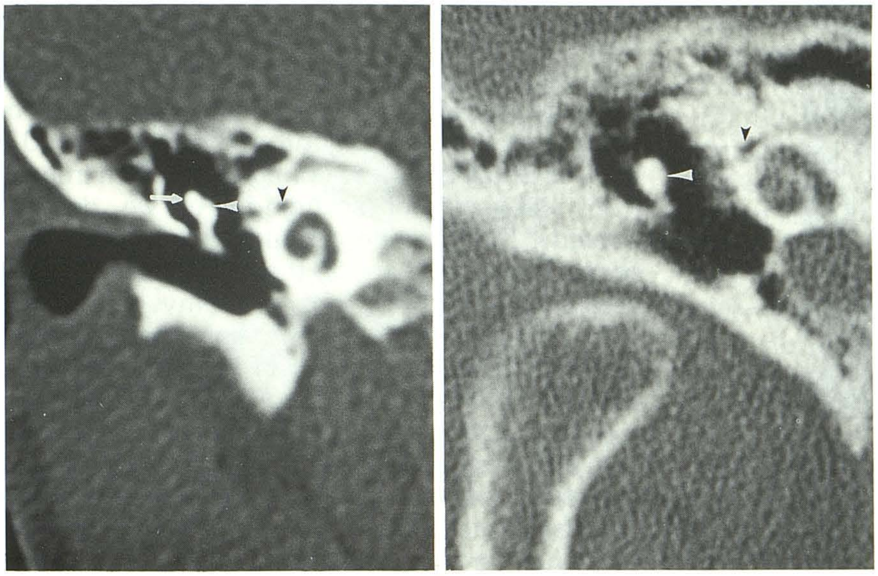

A B

Fig. 2. Comparison of direct coronal scans displaying the head of the malleus (*white arrowhead*), body of the incus (*white arrow*), and labyrinthine portion of the facial nerve canal (*black arrowhead*).

A, Spiral technique (1.25-mm effective section thickness).

B, Conventional technique (1-mm section thickness). The resolution is comparable between the two techniques.

loss of overall bone detail relative to conventional coronal scans. However, the ossicles, oval window, and second portion of the facial nerve canal were consistently identified. The sagittal reconstructions demonstrated the third part of the facial nerve canal, and gross ossicular relationships. Overall, a more prominent loss of anatomic detail was noted in sagittal reconstructions using the current algorithm. The resolution of the coronal and sagittal reconstructions using 180° linear interpolation was subjectively superior to the 360° algorithm and was comparable to direct scans (Fig 5).

Three-dimensional reconstructions in six patients always clearly displayed the oval window, malleus, and incus. Because of the restrictive thresholding algorithm employed in the 3D program, the entire stapes could not be demonstrated on a single image (Fig 6). Similarly, the margins of the ossicles and associated bones in the middle ear showed some loss of continuity. The bone detail and thresholding restrictions of the 3D reconstructions from submillimeter data were similar to those found using 1-mm sections.

Fig. 3. Spiral direct coronal scan (1.25-mm effective section thickness) showing soft tissue in the middle ear from a rhabdomyosarcoma. Bone destruction from this malignancy is present (*white arrowhead*). Also noted is the second turn of the cochlea (*large black arrowhead*) and the tympanic portion of the facial nerve canal (*small black arrowhead*).

Discussion

In the pediatric population, sedation is often required to complete conventional CT imaging of the temporal bone without patient motion. Our study shows the feasibility of performing spiral CT in all patients without sedation, irrespective of age. This study also used a lower x-ray technique (in milliamperes) than that used for conventional CT scans of the temporal bone, allowing a reduction in the radiation dosage. Previous studies have quantitatively and qualitatively demonstrated an increase in image noise with a lower-milliampere scan (4, 5). This is most notable in distinguishing small differences in soft-tissue attenuation. However, the diagnostic utility of CT scans is maintained until less than 40 mA are used (4, 5). Similar to prior studies involving low-dose CT of the paranasal sinuses, the presence of soft tissue is most often the pertinent finding in the temporal bone (4). Further characterization of these soft-tissue lesions based on subtle attenuation differences is seldom necessary to define temporal bone pathology.

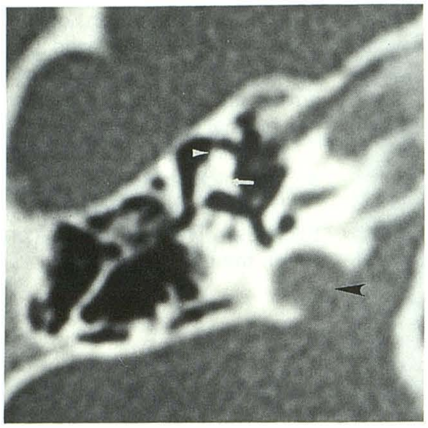

Fig. 4. Submillimeter (1.0-mm effective section thickness) axial image of the malleus (*white arrowhead*) and incus (*white arrow*) with spiral technique. The jugular fossa is also noted (*black arrowhead*).

Overall, the resolution of the spiral scans is subjectively comparable to conventional scans, and all pathologic lesions detected by conventional CT were demonstrated by spiral CT. However, direct visual comparisons of conventional images with the standard 360° linear-interpolation spiral images show diminished z-axis resolution for the spiral technique. The spiral CT technique collects data in a continuous fashion, rather than in discrete blocks as with conventional CT. Axial reconstructions made from the full 360° spiral inherently have broadening of the section sensitivity profile along the z axis (6–8). In this study, the table increment speed of 1 mm/second generates a theoretical section thickness of 1.00 mm; however, an effective section thickness of 1.25 mm results from 360° linear interpolation. The thicker slices may account for the diminished z-axis resolution of the 360° interpolation relative to conventional CT.

Because data are acquired continuously with spiral CT, images can be reconstructed using part of the 360° spiral. One hundred eighty-degree linear interpolation uses a subset of the full spiral to create images with an effective section thickness of less than 1.25 mm (8). In this study, sections with an effective thickness of 1.0 mm were generated from 180° linear interpolation; the images from this algorithm overlapped by 0.2 mm, as opposed to the contiguous 1-mm images from conventional scanning. As we demonstrated, these image features subjectively improve the resolution of the ossicles and other details of temporal bone anatomy. Compared with conventional CT, 180° linear-interpolation increases noise by a factor of 1.12 (8); however, this was not visible in our comparison of images. Although further experience is necessary to evaluate this technique fully, our initial work shows the 180° linear-interpolation images to be a highly promising method for assessing subtle middle- and inner-ear abnormalities.

Previous authors have discussed the value of direct multiplanar conventional CT in temporal bone imaging (9). The superior resolution of direct images versus multiplanar reconstructions has been emphasized. However, additional scanning planes increase the examination time and total radiation dose. Because of these problems, Lee et al (10) advocated the use of low-milliampere, high-resolution conventional axial images with multiplanar reconstructions. This latter technique demonstrated disease excellently. Our current work with low-radiation-dose spiral CT also demonstrates the effectiveness of multiplanar reconstructions in demonstrating disease while minimizing radiation exposure. The coronal reconstructions (360° linear interpolation) from axial spiral data are not as detailed as direct scans, but all the pertinent internal-ear anatomy and disease were delineated. When 180° linear interpolation is used, the image sections overlap by 0.2 mm; multiplanar reconstructions from this technique have significantly increased resolution and are comparable to the direct coronal examinations. We believe that multiplanar reconstructions using

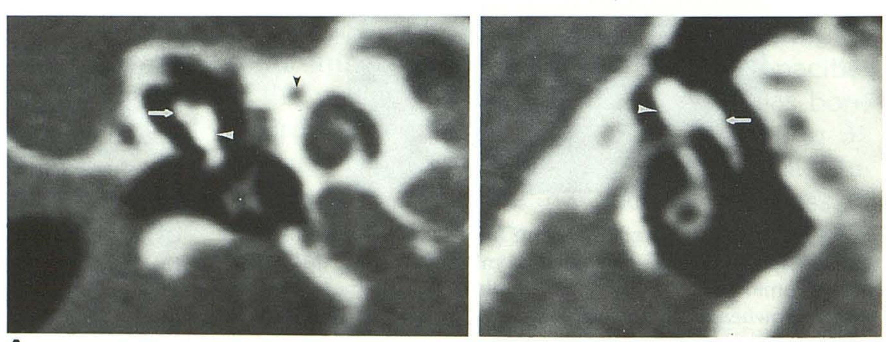

A B

Fig. 5. Submillimeter (1.0-mm effective section thickness) reconstructions (malleus = *white arrowhead*, incus = *white arrow*, and labyrinthine portion of the facial nerve canal = *black arrowhead*) from axial spiral data. *A*, Coronal. *B*, Sagittal.

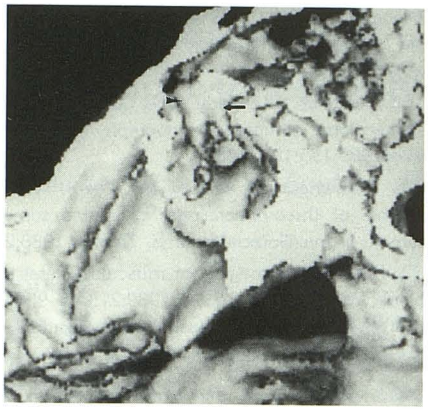

Fig. 6. Three-dimensional reconstruction of the ossicles from 1-mm axial spiral data. The malleus (*black arrowhead*) and incus (*black arrow*) are clearly demonstrated, but discontinuity of the bone margins is noted.

submillimeter axial data provide an alternative to direct scans in coronal and sagittal planes. As a result, direct multiplanar scanning can be avoided, and the overall radiation dosage to the lens is decreased.

Three-dimensional reconstructions have been used for temporal bone-surface anatomy (3). Programs for such reconstructions have been recently reviewed (11). These 3D renderings have been generated from conventional single-section CT scans. Because of the delay after each conventional scan, patient motion can occur between contiguous sections. Such motion causes misregistration between adjacent sections, degrading the spatial relationships and detail of the 3D reconstructions; this would be a significant limitation in unsedated pediatric patients. Spiral CT limits the potential for patient motion because of the reduced scanning time. The spiral CT technique also provides continuous data points rather than separate contiguous sections as with conventional CT. As a result, 3D reconstructions from the spiral data more accurately reflect the actual temporal bone anatomy. Our work confirms that high-quality 3D images of temporal bone internal anatomy can be constructed from spiral CT data.

In this study, we used a surface-rendering 3D program that employs a user-selected threshold value for image reconstruction. Our threshold value of 180 HU was empirically selected to depict optimally the osseous structures, particularly the ossicles. This value is comparable to that described by Howard et al (3). Three-dimensional images of middle-ear structures have problems similar to those reported for 3D reconstructions of temporal bone surface anatomy. Thin bones, such as the ossicles, are volume averaged with the adjacent soft tissues; the resultant pixel has a CT number that is less than the threshold value (9). Such pixels are discarded from the 3D reconstruction, creating bone depletion artifacts. Because the original data set remains constant, these artifacts are present with both the 180° and 360° interpolations. Increasing the threshold value worsens this loss of pixels. Conversely, a decrease in threshold allows excessive soft tissue and noise to be included along with the bone, thus reducing bone detail. In our work, such artifacts cause an incomplete representation of the stapes.

For the middle and inner ear, 3D imaging is most useful in globally depicting the interrelationships of the ossicles and oval window. A similar role has been ascribed to 3D imaging of other osseous structures (12–15). Although we did not encounter any cases of ossicular disruption in our series, 3D imaging in this setting is potentially useful in surgical planning. However, 3D imaging of the middle and inner ear structures remains complementary to the standard 2D renditions.

In summary, we have demonstrated that the spiral CT technique is an effective method for evaluating the temporal bone in pediatric patients. Because the scans are completed in 30 seconds, sedation is not needed even in very young patients. The spiral scans, both direct axial and coronal, are comparable in resolution to conventional CT techniques. From this same spiral data, high-quality multiplanar and 3D reconstructions can be obtained.

Acknowledgments

We appreciate the capable technical assistance of Roberta Yoffie, RT, and Barry Brurusden. Technical advice and engineering assistance from Willi Kalendar, PhD, and Alexander Polacin, PhD, of Siemens-Erlangen are gratefully appreciated.

References

1. Swartz JD. Current imaging approach to the temporal bone. *Radiology* 1989;71:309–317
2. Howard JD, Elster AD, May JS. Temporal bone: three-dimensional CT. Part II. Pathologic alterations. *Radiology* 1990;177:427–430
3. Howard JD, Elster AD, May JS. Temporal bone: three-dimensional CT. Part I. Normal anatomy, techniques, and limitations. *Radiology* 1990;177:421–425
4. Marmolya G, Wiesen EJ, Yagan R, Haria CD, Shah AC. Paranasal sinuses: low-dose CT. *Radiology* 1991;181:689–691
5. Haaga JR, Miraldi F, Macintyre W, LiPuma JP, Bryan PJ, Wiesen EJ. The effect of mAs variation upon computed tomography image quality as evaluated by in vivo and in vitro studies. *Radiology*

1981;138:449–454
6. Kalender WA, Polacin A. Physical performance characteristics of spiral CT scanning. *Med Phys* 1991;18:910–915
7. Polacin A, Kalender WA, Marchal G. Evaluation of section sensitivity profiles and image noise in spiral CT. *Radiology* 1992;185:29–35
8. Kalender W, Polacin A, Marchal G, Baert AL. Current status and new perspectives in spiral CT. In: Felix R, Langer M, eds. *Advances in CT II: Second European Scientific User Conference*. Berlin: Springer-Verlag, 1992:87–94
9. Mafee MF, Kumar A, Tahmoressi CN, et al. Direct sagittal CT in the evaluation of temporal bone disease. *AJNR: Am J Neuroradiol* 1988;9:371–378
10. Lee BCP, Black ML, Lamb RB, et al. CT evaluation of the temporal bone ossicles by using oblique reformations. A technical note. *AJNR: Am J Neuroradiol* 1989;10:431–433
11. Fishman EK, Magid D, Ney DR, et al. Three-dimensional imaging. *Radiology* 1991;181:321–337
12. Burk DL, Mears DC, Kennedy WH, Cooperstein LA, Herbert DL. Three-dimensional computed tomography of acetabular fractures. *Radiology* 1985;155:183–186
13. Mayer JS, Wainwright DJ, Yeakley JW, Lee KF, Harris JH, Kulkarni M. The role of three-dimensional computed tomography in the management of maxillofacial trauma. *Trauma* 1988;28:1043–1053
14. Magid D, Fishman E. Imaging of musculoskeletal trauma in three dimensions. *Radiol Clin North Am* 1989;27:945–956
15. Vannier MW, Totty WG. Musculoskeletal applications of three dimensional surface reconstructions. *Orthop Clin North Am* 1985;16:543–555